Complete Higgs sector constraints on dimension-6 operators

John Ellis,[a,b] **Verónica Sanz**[c] **and Tevong You**[a]

[a]*Theoretical Particle Physics and Cosmology Group, Physics Department,*
King's College London, London WC2R 2LS, U.K.

[b]*TH Division, Physics Department, CERN,*
CH-1211 Geneva 23, Switzerland

[c]*Department of Physics and Astronomy, University of Sussex,*
Brighton BN1 9QH, U.K.

E-mail: john.ellis@cern.ch, v.sanz@sussex.ac.uk, tevong.you@kcl.ac.uk

Abstract: Constraints on the full set of Standard Model dimension-6 operators have previously used triple-gauge couplings to complement the constraints obtainable from Higgs signal strengths. Here we extend previous analyses of the Higgs sector constraints by including information from the associated production of Higgs and massive vector bosons (H+V production), which excludes a direction of limited sensitivity allowed by partial cancellations in the triple-gauge sector measured at LEP. Kinematic distributions in H+V production provide improved sensitivity to dimension-6 operators, as we illustrate here with simulations of the invariant mass and p_T distributions measured by D0 and ATLAS, respectively. We provide bounds from a global fit to a complete set of CP-conserving operators affecting Higgs physics.

Contents

1 Introduction

The investigation of the properties of the recently-discovered Higgs boson [1, 2] proceeded initially by characterizing its signal strength relative to the Standard Model (SM) expectation [3, 4], with many studies refining this picture to constrain deviations in the Higgs couplings under various assumptions [5–44]. Although the signal strengths and pattern of couplings provided some information about the spin and parity of the Higgs boson [45], it was through the use of differential kinematic distributions that different Lorentz structures could be probed most thoroughly [46–70]. The evidence now indicates convincingly [71–73] that we are dealing with a spin-zero, positive-parity particle, as expected for the Higgs boson responsible for electroweak symmetry breaking.

Moreover, there is no significant indication of any deviation of the dimension-4 couplings of this particle from those expected in the SM. Studies of these couplings continue, and are being supplemented by searches for anomalous couplings that could arise from new physics in the electroweak sector. If this new physics is decoupled at some heavy scale, then the effects of these interactions are cohesively captured by supplementing the SM Lagrangian with higher-dimensional operators involving multiple fields and/or derivative interactions in an effective field theory (EFT) framework[1] [74–78].

---

[1]For a recent short review, see [79].

Constraints on these operators have been placed for subsets of operators [80–89] and in full global fits both before [90] and after [91–93] the Higgs discovery.[2] Many strong constraints come from electroweak precision tests (EWPT) [94–96] at LEP, and from triple-gauge coupling (TGC) [91, 92, 97] measurements at LEP and the LHC. In the case of Higgs observables, aside from operators contributing to couplings that are absent at tree-level in the SM, only weaker limits are available so far. Some combinations of these operators enter into EWPT and TGC, but the presence of a poorly constrained direction [98] in measurements of the latter means that constraints on dimension-6 operators from Higgs physics are complementary and not redundant within the EFT framework. Constraints from EWPT on operators that contribute at loop level rely on assuming no unnatural cancellations [99–105], with unambiguous bounds being far weaker [106, 107]. Thus, it is desirable to refine as much as possible the analysis of the Higgs sector [108].

We illustrate here the power of associated $H + V$ production and its differential kinematic distributions to constrain CP-conserving dimension-6 operators within the EFT framework. In particular, we note that the distribution of the $H + V$ invariant mass, m_{VH}, measured by D0 [109] and the vector-boson transverse momentum, p_T^V, distribution measured by ATLAS [110] in the associated production channel $V + H \to V\bar{b}b$ have very low backgrounds in the higher mass and p_T bins, respectively, where higher-dimension operators would contribute. These searches are, therefore, ideal for constraining the boosted signature of new physics that could arise from dimension-6 operators, despite the large uncertainties in the total signal strength [111, 112]. Moreover, we find that the inclusion of associated production at D0 and ATLAS removes certain degeneracies in a complete fit to the full set of operators affecting Higgs physics.

In the following section we introduce the CP-even dimension-6 operators that affect Higgs physics. In section 3.1 we constrain one operator using the m_{VH} distribution of $VH \to V\bar{b}b$ in the $V \to$ 0-, 1- and 2-lepton sub-channels used in the D0 search, quantifying the improvement obtained by using differential information, and we do the same using the ATLAS p_T^V distribution in section 3.2. In section 4 we combine these channels and make a multi-parameter fit to obtain global constraints from the Higgs sector. Section 5 summarizes our conclusions. Details of the analysis implementations for D0 and ATLAS can be found in the appendices.

2 Dimension-6 operators in the Higgs sector

In the basis of [113–116], the CP-even dimension-6 Lagrangian involving Higgs doublets may be written as

$$\mathcal{L} \supset \frac{\bar{c}_H}{2v^2} \partial^\mu [\Phi^\dagger \Phi] \partial_\mu [\Phi^\dagger \Phi] + \frac{g'^2 \, \bar{c}_\gamma}{m_W^2} \Phi^\dagger \Phi B_{\mu\nu} B^{\mu\nu} + \frac{g_s^2 \, \bar{c}_g}{m_W^2} \Phi^\dagger \Phi G_{\mu\nu}^a G_a^{\mu\nu}$$

$$+ \frac{2ig \, \bar{c}_{HW}}{m_W^2} [D^\mu \Phi^\dagger T_{2k} D^\nu \Phi] W_{\mu\nu}^k + \frac{ig' \, \bar{c}_{HB}}{m_W^2} [D^\mu \Phi^\dagger D^\nu \Phi] B_{\mu\nu}$$

---

[2]Ref. [93] in particular includes a full set of operators in the EWPT sector.

$$+\frac{ig\,\bar{c}_W}{m_W^2}\big[\Phi^\dagger T_{2k}\overleftrightarrow{D}^\mu\Phi\big]D^\nu W_{\mu\nu}^k + \frac{ig'\,\bar{c}_B}{2m_W^2}\big[\Phi^\dagger\overleftrightarrow{D}^\mu\Phi\big]\partial^\nu B_{\mu\nu}$$

$$+\frac{\bar{c}_t}{v^2}y_t\Phi^\dagger\Phi\ \Phi^\dagger\cdot\bar{Q}_L t_R + \frac{\bar{c}_b}{v^2}y_b\Phi^\dagger\Phi\ \Phi\cdot\bar{Q}_L b_R + \frac{\bar{c}_\tau}{v^2}y_\tau\ \Phi^\dagger\Phi\ \Phi\cdot\bar{L}_L\tau_R\,. \tag{2.1}$$

We note that $\bar{c}_T$ corresponds to the $\hat{T}$ parameter, which is constrained at the per-mille level by EWPT, and $\bar{c}_6$ only affects the Higgs self-coupling, so we drop these from our analysis. The linear combination $\bar{c}_W + \bar{c}_B$ is related to the $\hat{S}$ parameter, which is also bounded at the per-mille level, so we set $\bar{c}_B = -\bar{c}_W$. The independent set of parameters affecting Higgs physics is thereby reduced to

$$\bar{c}_i \equiv \{\bar{c}_H, \bar{c}_{t,b,\tau}, \bar{c}_W, \bar{c}_{HW}, \bar{c}_{HB}, \bar{c}_\gamma, \bar{c}_g\}\,. \tag{2.2}$$

The other dimension-6 operators enter either in EWPT or TGC observables, but do not affect the Higgs sector. For an analysis of the above operators and TGCs, see ref. [91, 92, 97].

A more phenomenological and experimentally transparent approach is often used in the form of an effective Lagrangian with anomalous Higgs couplings. Experimental bounds expressed in terms of anomalous couplings may then be related to other more theoretically-motivated effective theories or models, which has proven to be a useful approach for EWPT and TGCs. For example, following ref. [117], the relevant subset of the Higgs anomalous couplings in the mass basis and unitary gauge includes

$$\begin{aligned}\mathcal{L} \supset\ & -\frac{1}{4}g_{HZZ}^{(1)}Z_{\mu\nu}Z^{\mu\nu}h - g_{HZZ}^{(2)}Z_\nu\partial_\mu Z^{\mu\nu}h \\ & -\frac{1}{2}g_{HWW}^{(1)}W^{\mu\nu}W_{\mu\nu}^\dagger h - \Big[g_{HWW}^{(2)}W^\nu\partial^\mu W_{\mu\nu}^\dagger h + \text{h.c.}\Big]\,,\end{aligned} \tag{2.3}$$

with the relation between these anomalous coupling coefficients and the dimension-6 coefficients in our basis given by

$$\begin{aligned}g_{hzz}^{(1)} &= \frac{2g}{c_W^2 m_W}\big[\bar{c}_{HB}s_W^2 - 4\bar{c}_\gamma s_W^4 + c_W^2\bar{c}_{HW}\big] \\ g_{hzz}^{(2)} &= \frac{2g}{c_W^2 m_W}\big[(\bar{c}_{HW} + \bar{c}_W)c_W^2 + (\bar{c}_{HB} + \bar{c}_B)s_W^2\big] \\ g_{hww}^{(1)} &= \frac{2g}{m_W}\bar{c}_{HW} \\ g_{hww}^{(2)} &= \frac{g}{m_W}(\bar{c}_W + \bar{c}_{HW})\,.\end{aligned} \tag{2.4}$$

We refer the reader to ref. [117] for more details and a complete list of Higgs anomalous couplings.

We calculate the effects of the dimension-6 operators on $V+H$ associated production by Monte-Carlo (MC) simulations using `MadGraph5 v2.1.0` [118] interfaced with `Pythia` [119] and `Delphes v3` [120], combined with the dimension-6 model implementation developed in [117]. We start with $\bar{c}_W$ as an illustrative example, switching off all other coefficients, before considering briefly $\bar{c}_{HW}$ and then the full set of coefficients (2.2) in a global fit.
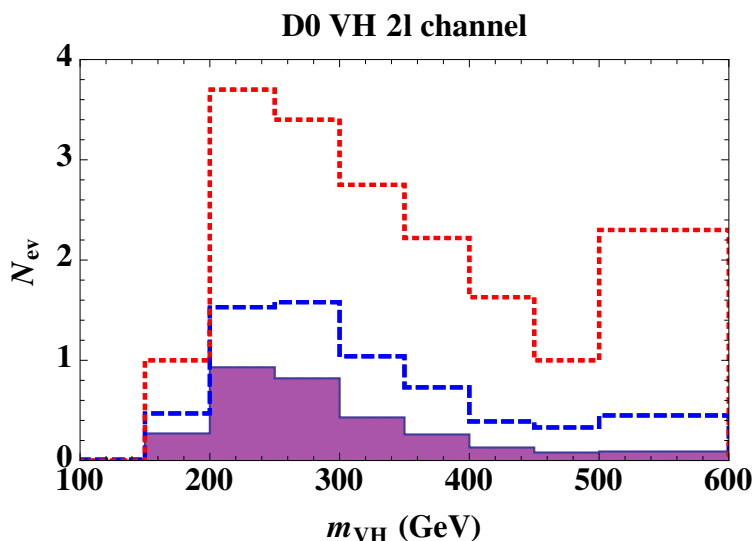
Figure 1. Simulation of the m_{VH} distribution in $(V \to 2\ell) + (H \to \bar{b}b)$ events at the Tevatron after implementing D0 cuts, obtained using `MadGraph v2.1.0` interfaced with `Pythia` and `Delphes v3`, combined with the dimension-6 model implementation developed in [117]. The solid distribution is the SM expectation, while the red-dotted and blue-dashed lines correspond to the distributions with $\bar{c}_W = 0.1$ and 0.035, respectively.

3 Kinematic distributions in $H + V$ production

3.1 The $H + V$ invariant mass distribution measured by D0

It was pointed out in [121], see also [111, 112], that the invariant mass distribution in $H + V$ events could be used to discriminate between minimally-coupled $J^P = 0^+, 0^-$ and graviton-like 2^+ spin-parity assignments for the H particle. Subsequently, the D0 Collaboration has made available the observed $H + V$ invariant mass distribution as well as those expected in these scenarios [109]. Here we use their background distribution and simulate the signal events for a SM Higgs including the effects of non-zero dimension-6 coefficients, considering separately the 2-, 1- and 0-lepton channels for the decays of vector bosons $V = Z, W^{\pm}$ produced in association with H decaying to $b\bar{b}$.

Implementation details of the simulation can be found in appendix A. Summing the cross-section times efficiency over the 0-, 1- and 2-lepton channels, we obtain the following signal strength as a function of $\bar{c}_W$ for $VH \to V\bar{b}b$ at D0,

$$\mu_{H\bar{b}b} \simeq 1 + 29\bar{c}_W,$$

indicating a strong dependence of the signal strength on the coefficient of the dimension-6 operator, which compensates for the relatively large error bar in the D0 measurement of this channel. We find that the best-fit signal strength $\mu_{H\bar{b}b} = 1.2 \pm 1.2$ reported by D0 [109] yields the following 95% CL bounds in a χ^2 fit:

$$\bar{c}_W \in [-0.15, 0.09].$$

More information can be obtained from the differential kinematic distribution for $H + V$ production by considering the measurements in bins in m_{VH}, which affords full sensitivity
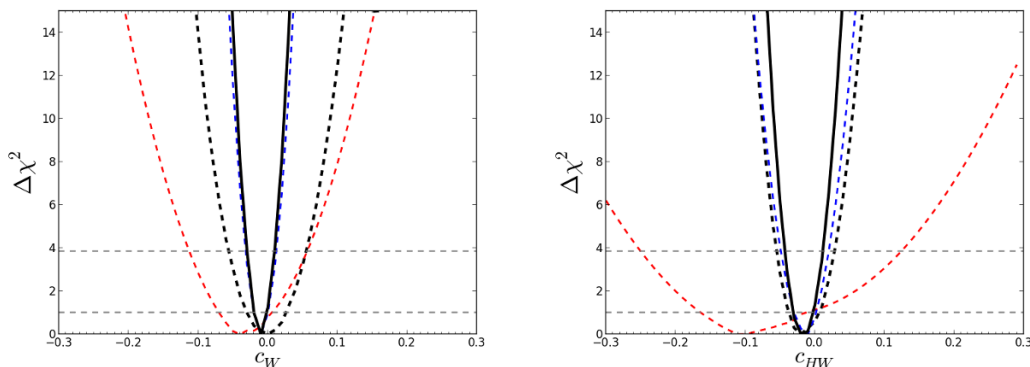
Figure 2. The one-dimensional fit to the parameter $\bar{c}_W$ (left panel) and to $\bar{c}_{HW}$ (right panel). In each panel, the dashed-red line corresponds to the constraint from the 0-, 1- and 2-lepton D0 m_{VH} distribution including all bins, the dashed-blue line to the 0-, 1- and 2-lepton ATLAS p_T^V distribution using the last bin only, the dashed-black is the combination of CMS and ATLAS signal strengths in all channels except VH, and the solid-black is the combination of all the above.

to $\bar{c}_W$ via the differential information available in the invariant mass distribution, particularly in the higher-mass bins where the signal-to-background ratio increases most rapidly. The invariant mass distribution found in our simulation is plotted for the 2-lepton case in figure 1 for various values of $\bar{c}_W$. As expected, the effect of the dimension-6 operator is to generate a larger tail at high invariant masses than in the SM.

We include the information from signal strength and differential distribution by constructing a χ^2 function with a contribution from each m_{VH} bin. We treat the errors provided as Gaussian, neglecting any correlations between bins as this information is not available. Since the sensitivity of the distribution analysis is largely driven by the last bin, the sensitivity of the limit to correlations is minimal. The resulting improved bounds are

$$\bar{c}_W \in [-0.11, 0.06].\tag{3.1}$$

The χ^2 distribution from this constraint is shown as the dashed-red line in the left panel of figure 2.

This limit, using differential information, is better than the more inclusive observable μ_{HV} by 15-20 %. A better understanding of the tail in the kinematic distribution could improve considerably this limit. However, the Tevatron analysis is limited by statistics, whereas the LHC experiments benefit from increased energy, which expands the available phase space and hence enhances the effect of anomalous couplings, with the prospect also of future improvements in statistical significance. The study of constraints from Run 1 of the LHC at 8 TeV is the subject of the next section.

3.2 The vector-boson transverse-momentum distribution measured by AT-LAS

The fact that dimension-6 operators generate a larger tail at higher invariant masses by modifying the production kinematics implies greater sensitivity at the LHC, where the higher energy opens up the available phase space. Since the $V + H$ invariant mass distribution is not available, we make use here of the transverse momentum of the vector boson,
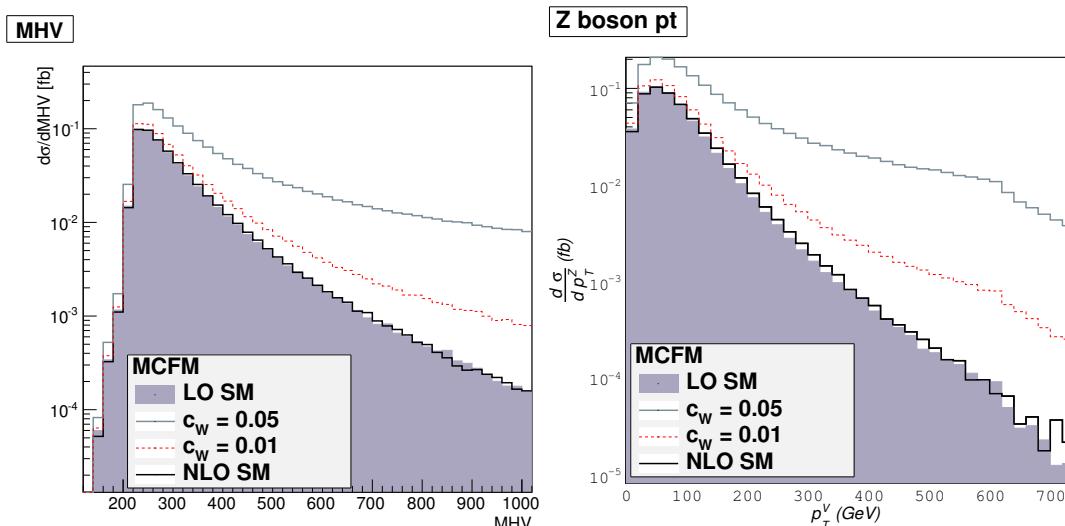
Figure 3. The invariant mass (left panel) and transverse momentum (right panel) distributions for LHC Run 1 at 8 TeV, calculated with LO and NLO QCD and compared with the effects of an effective operator.

p_T^V, measured by ATLAS. However, the p_T^V distribution is more affected by NLO QCD corrections than is the $V + H$ invariant mass distribution [122]. We present in figure 3 the results of an NLO calculation using MCFM [123–125]. Although the p_T^V distribution is more sensitive to NLO corrections, the constraint on the coefficient of an effective operator that we can obtain with LHC Run 1 data at 8 TeV is still quite insensitive to the QCD higher order corrections. However, this will be an important effect when reaching $\bar{c}_W \sim \mathcal{O}(10^{-3})$. Since such effects tend to broaden the p_T^V distribution in the SM, the inclusion of NLO would only strengthen the bounds reported here and as such will not modify our conclusions, which are reached under conservative assumptions.

Details of the cuts implemented for the 0-,1- and 2-lepton ATLAS analysis can be found in appendix B. Figure 4 is an example of the p_V^T distribution for the 2-lepton signal in the bins used by the ATLAS search, for various values of $\bar{c}_W$.

We see that the number of events in the last (overflow) bin increases rapidly with $\bar{c}_W$. Since the background overwhelms any signal in the lower bins, henceforth we focus exclusively on this overflow bin where the signal-to-background ratio is highest. A χ^2 fit to the observed data gives the 95% CL range

$$\bar{c}_W \in [-0.07, 0.07],$$

which improves upon the D0 constraint (3.1), as expected. The contribution to the χ^2 function from this constraint is shown as the dashed blue line in the left panel of figure 2. For comparison, using the signal strength given for each of the 0-, 1- and 2-lepton channels, which grow with $\bar{c}_W$ as

$$\mu_{2-\text{lepton}} \simeq 1 + 23\bar{c}_W$$
$$\mu_{1-\text{lepton}} \simeq 1 + 32\bar{c}_W$$
$$\mu_{0-\text{lepton}} \simeq 1 + 33\bar{c}_W,$$
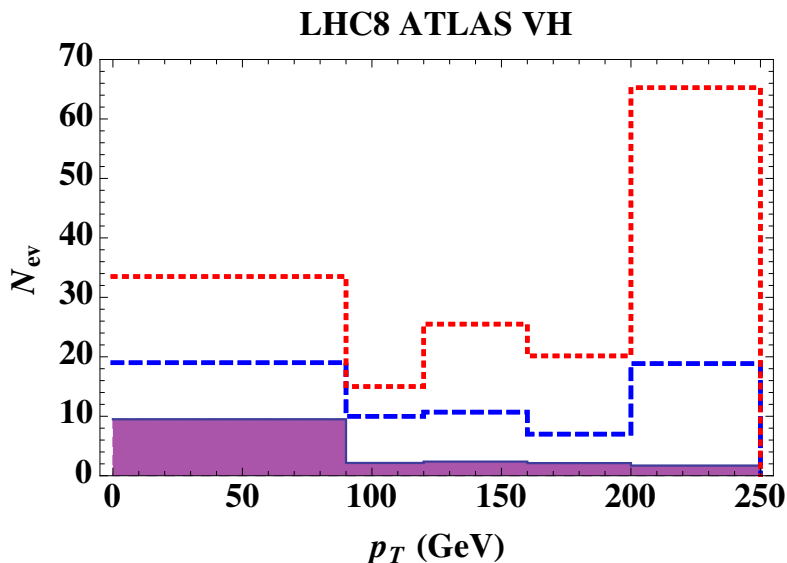
Figure 4. Simulation of the p_T^V distribution in $(V \to 2\ell) + (H \to b\bar{b})$ events at the LHC after implementing ATLAS cuts, as obtained using `MadGraph v2.1.0` interfaced with `Pythia` and `Delphes v3`, combined with the dimension-6 model implementation developed in [117]. The solid distribution is the SM expectation, and the red-dotted and blue-dashed lines correspond to the distributions with $\bar{c}_W = 0.1$ and 0.05, respectively.

we find the 95% CL range

$$\bar{c}_W \in [-0.09, 0.03],$$

which is comparable to that using only the last bin of the p_V^T differential distribution.

We emphasise that only the leading linear dependence on the dimension-6 coefficient is kept in our fit. Including the quadratic term could appear to give tighter constraints as it allows the signal to grow faster with increasing $\bar{c}_W$, but such bounds are spurious since it is not consistent to include a dependence on $\bar{c}_W^2$ without also introducing dimension-8 operators whose effects are formally of the same order. In the example given above, including the quadratic term would reduce the bounds to $[-0.06, 0.03]$ for the signal-strength fit and $[-0.04, 0.04]$ for the binned fit. This sensitivity to higher-order effects indicates the level to which we may trust these constraints. At the current level of precision, the differences in the bounds between the linear and quadratic fits are larger than any uncertainties in background distributions or MC simulations.

Full results of one-dimensional fits for $\bar{c}_W$ are summarized on the left plot in figure 2. In addition to the dashed red line corresponding to the analysis of the D0 m_{VH} distribution and the dashed blue line corresponding to the ATLAS p_T^V distribution discussed above, the dashed black line is the combination of CMS and ATLAS signal strengths including all channels except VH, and the solid black line is the combination of all the above. The right panel of figure 2 shows the corresponding one-dimensional constraints on $\bar{c}_{HW}$, where we see that the addition of the differential information is less important than for $\bar{c}_W$.

4 Global constraints from signal strengths and differential distributions

Following these examples, we now combine the information from associated production measurements in the $H \to \bar{b}b$ final state by D0 and ATLAS together with the signal strengths in the $H \to \gamma\gamma, \gamma Z, WW, ZZ$ and $\tau\tau$ search channels measured by CMS and ATLAS. We first constrain the dimension-6 coefficients individually, setting to zero all other coefficients, and then include the full set of coefficients (2.2) in a global fit.

The decay widths for $H \to Z^*Z^{(*)} \to 4l$, $H \to W^*W^{(*)} \to l\nu l\nu$, $H \to \bar{f}f$, $H \to gg$ and $H \to \gamma\gamma$ have dependences on the dimension-6 coefficients that are given in [126, 127]. The dimension-6 operators also affect the vector boson fusion (VBF) production mode. Using the standard VBF cuts used at the LHC 8-TeV analysis, namely $m_{jj} > 400\,\mathrm{GeV}$, $p_T^j > 20\,\mathrm{GeV}$, $|\eta_j| < 4.5$ and $\Delta\eta_{jj} > 2.8$, we find

$$\frac{\sigma(pp \to V^*V^*jj \to hjj)}{\sigma(pp \to V^*V^*jj \to hjj)_{\mathrm{SM}}} \simeq 1 - 8.30(\bar{c}_W + \tan^2\theta_w \bar{c}_B) - 6.9(\bar{c}_{HW} + \tan^2\theta_w \bar{c}_{HB}) - 0.26\bar{c}_\gamma\,.$$

We confront these predictions with the likelihoods for the total signal strengths μ given by ATLAS and CMS in a particularly useful form [128] as a 2-dimensional χ^2 grid of $\mu_{\mathrm{ggF,\,tth}}$ vs $\mu_{\mathrm{VBF,AP}}$. For ATLAS we use the likelihoods made publicly available for diboson final states in [129] and the 2-dimensional $H \to \tau\tau$ likelihood given in [130]. The CMS likelihoods for the $H \to \gamma\gamma, WW^*, ZZ^*$ and $\tau\tau$ channels are taken from [131]. We assume gluon fusion and VBF to be the dominant production modes in all these channels, with associated production only entering the fit through the differential distributions of the D0 and ATLAS $\bar{b}b$ final states.[3] The $H \to Z\gamma$ likelihood is reconstructed from the expected and observed 95% CL signal strength using the method of [132].

The result of the signal strength fit for all channels excluding $\bar{b}b$ at ATLAS and CMS gives the following 95% CL range for $\bar{c}_W$, setting all other coefficients to zero:

$$\bar{c}_W \in [-0.05, 0.06]\,.$$

Including the ATLAS p_V^T and D0 m_{VH} information discussed in the previous section reduces this range to

$$\bar{c}_W \in [-0.03, 0.01]\,.$$

The improvement of the limit on a single operator is significant. Furthermore the importance of using as many inputs as possible becomes clear when one includes several operators simultaneously [89]. For example, allowing the coefficient $\bar{c}_{HW}$ to vary simultaneously with $\bar{c}_W$ introduces a possible degeneracy in the fit, as shown in the upper left panel of figure 5. We see that the D0 m_{VH} data alone constrain essentially just one linear combination of $\bar{c}_W$ and $\bar{c}_{HW}$, and a similar effect occurs in the upper right panel where the result of a 2-parameter fit to just the ATLAS p_T^V data is shown. However, the correlation coefficients are somewhat different, so that combining the two sets of data breaks the degeneracy to some extent, as seen in the lower left panel of figure 5. Finally, in the lower right panel

---

[3]The signal strength information is also included in the differential distribution through the normalisation of the heights of each bin to the total number of signal events.
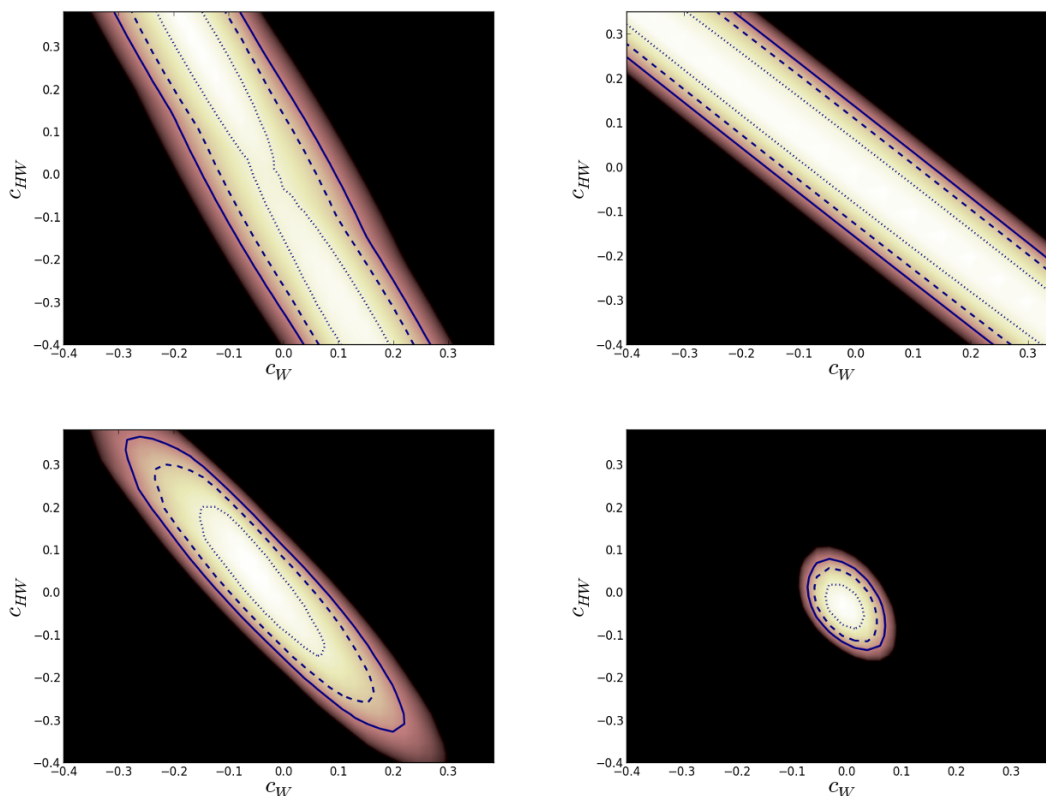
Figure 5. Regions in the $(\bar{c}_W, \bar{c}_{HW})$ planes allowed at the 68 (95) (99)% CL (in lighter shading and bounded by dotted, dashed and solid lines, respectively) in fits to the D0 m_{VH} data alone (upper left panel), the ATLAS p_T^V data alone (upper right panel), the combination of these data (lower left panel) and a global fit using also signal-strength information from CMS and ATLAS (lower right panel).

of figure 5 the degeneracy between $\bar{c}_W$ and $\bar{c}_{HW}$ is completely removed when the D0 and ATLAS associated production data are combined with the signal strength data from the other channels. This is primarily because, of the two operators considered here, only $\bar{c}_W$ enters in the $H \to \gamma\gamma$ decay width.

Finally we consider the full set of 8 dimension-6 operators listed in (2.2), setting $c_b = c_\tau \equiv c_d$, including a linear dependence on these coefficients in the ATLAS and CMS signal strengths, combined with the differential distribution information of $H + V$ associated production at ATLAS and D0 discussed in section 3. The result of a scan over the 8-dimensional parameter space is represented by the marginalized $\Delta\chi^2$ in solid black in figure 6. The blue dashed line in figure 6 is the result of the 8-parameter fit using only ATLAS and CMS signal strengths without $H + V \to V\bar{b}b$ associated production information. We see that omitting associated production yields no significant constraints on any of the operators aside from $\bar{c}_g$.[4]

---

[4]The bi-modal distribution of $\bar{c}_g$ is due to the linear dependence on the coefficient of the gluon production cross-section rescaling, which is not allowed to go negative and so is responsible for the two minima in the best fit.
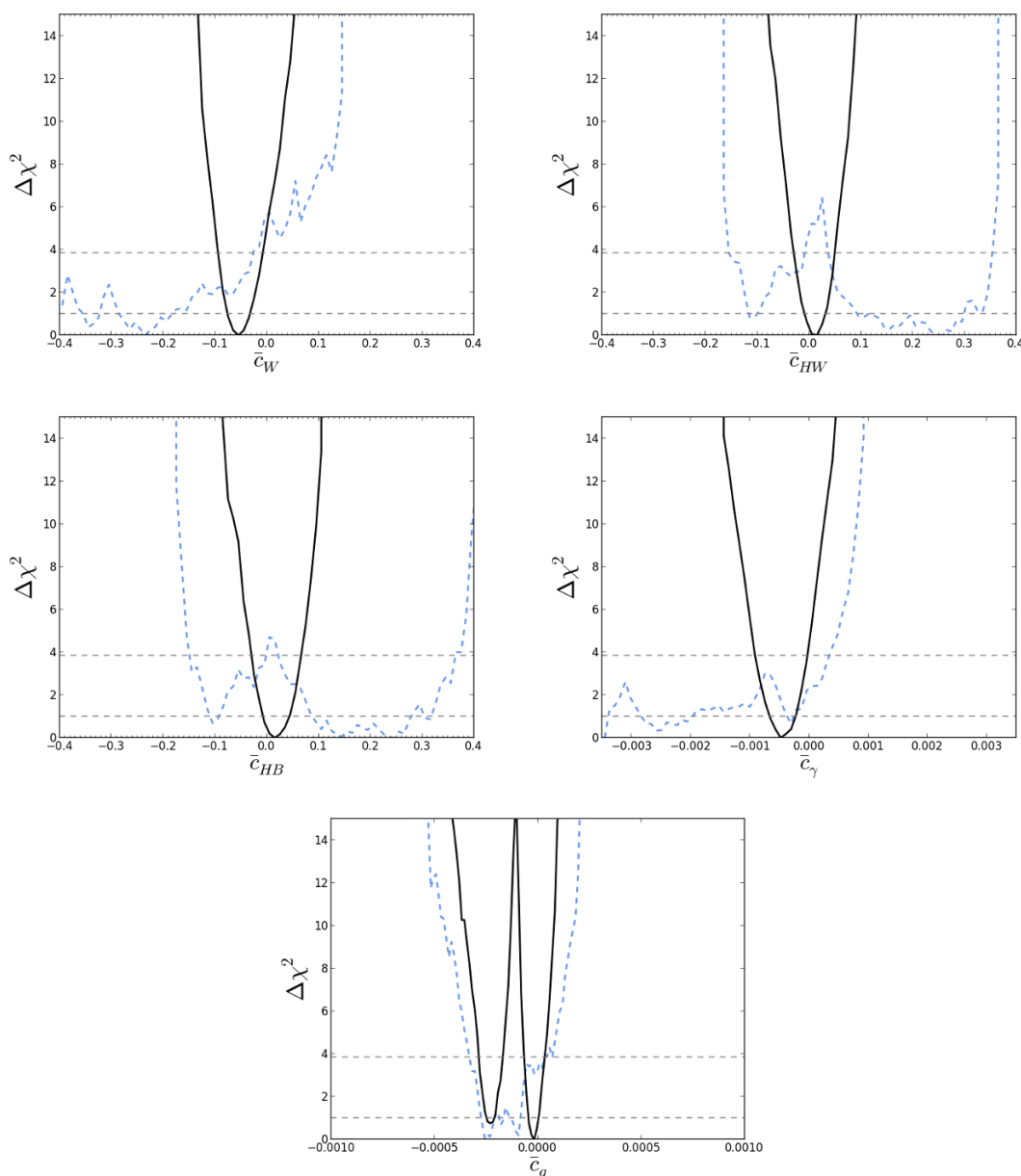
Figure 6. Marginalized $\Delta\chi^2$ from a scan over the 8-dimensional parameter space (2.2) using the differential distribution information about $H + V$ associated production from D0 and ATLAS as well as the ATLAS and CMS signal strengths (solid black line) and dropping the information from the kinematic distributions (blue dashed line).

The scan over the 8-dimensional parameter space including the kinematical information from $H + V$ production yields the 95% CL bounds summarized in the black error bars of figure 7. Also shown in green in figure 2 are the 1-dimensional constraints obtained by switching on one operator at a time with all others set to zero. We omit c_t, c_d and c_H in this and the previous figure, as no meaningful constraints are found for these coefficients.
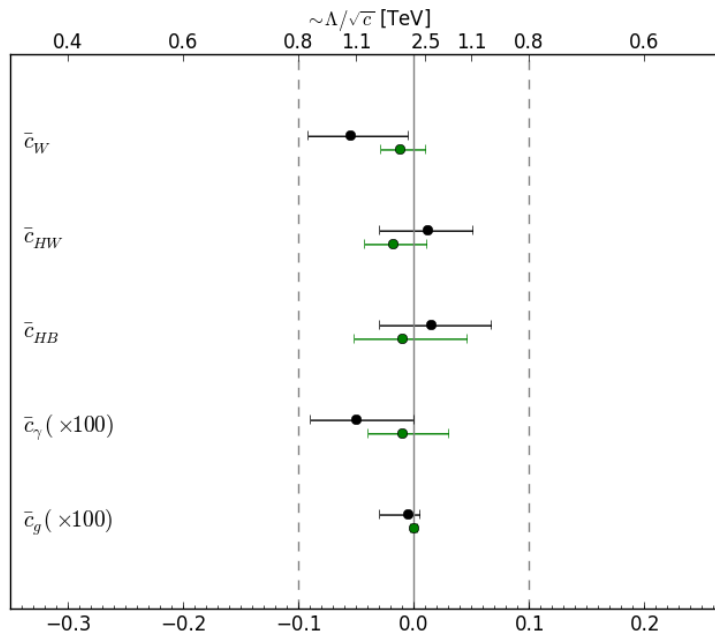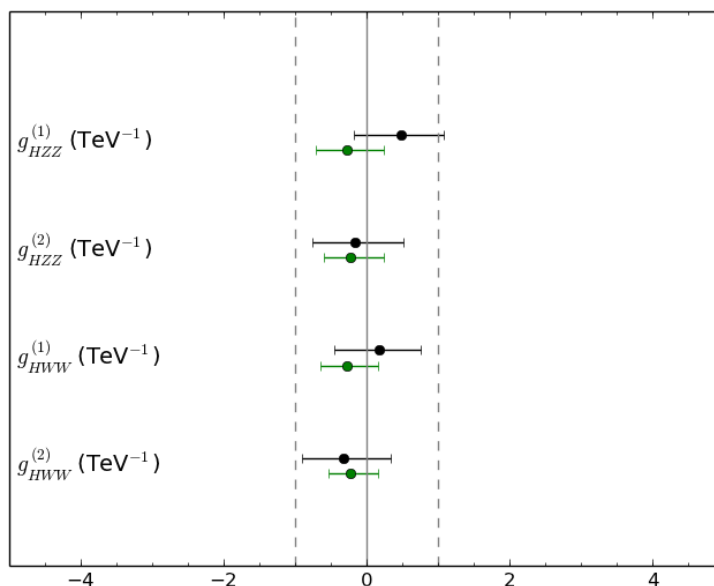
Figure 7. The 95% CL ranges allowed in a global fit to the dimension-6 operator coefficients listed in (2.2) (black), and the 95% CL ranges allowed for each operator coefficient individually, setting the others to zero (green). The upper axis is the corresponding sensitivity to the scale $\Lambda/\sqrt{c}$ in TeV where $\bar{c} \equiv c\frac{v^2}{\Lambda^2}$. Note that $\bar{c}_{\gamma,g}$ are shown $\times 100$ for which the upper axis should therefore be read $\times 10$.

We may also express the bounds obtained here in terms of the Higgs anomalous couplings as parametrized in (2.3). Our results are displayed in figure 8 using the same colour coding as in figure 7.

5 Conclusions

With Higgs property measurements consistent with SM expectations, and no clear sign of new physics from Run I of the LHC, it is natural to consider the SM as an effective theory supplemented by dimension-6 operators whose effects are suppressed by the scale of new physics. In this model-independent approach it is particularly interesting to consider a complete set of operators that minimizes any assumptions on the Wilson coefficients one chooses to include, thus providing truly universal bounds if one accepts the framework of the SM and decoupled new physics.

In this analysis we considered the set of CP-even operators that affect the Higgs sector at tree-level. Certain operators contain derivative interactions that modify the kinematics in $H + V$ associated production, modifying in particular the tail in the differential distribution of the $V + H$ invariant mass and the vector boson transverse momentum. We simulated the $V + H \rightarrow V b\bar{b}$ process at D0 and found greater sensitivity to dimension-6 operators using the differential invariant mass distribution than using only signal strength information in this channel. Since the higher energies of the LHC enlarge the available

Figure 8. The 95% CL ranges allowed in a global fit to the anomalous Higgs couplings listed in (2.4) (black), and the 95% CL ranges allowed for each coupling individually, setting the others to zero (green).

phase space for boosted new physics, observations of the same process by ATLAS and CMS are expected to be more sensitive than D0 to the effects of dimension-6 operators, as we have confirmed here. Moreover, including kinematic distributions from both Tevatron and LHC can help remove degeneracies in multi-parameter fits.

Including differential distributions of associated production with the signal strength from other channels, we have performed a scan of the 8-dimensional parameter space of the CP-even dimension-6 operator coefficients and placed 95% CL bounds. Without the use of associated production information, there are degeneracies that give flat directions in the fit. These could otherwise be eliminated using measurements of TGCs. However, this may introduce model-dependent assumptions as TGCs, despite their greater sensitivity compared to Higgs measurements, also contain a poorly constrained direction due to a partial cancellation among contributions to $e^+e^- \to W^+W^-$. Thus the use of associated Higgs production complements other ingredients in global fits to a complete set of operators. As better measurements of TGCs at the LHC become available it will be interesting to fully explore this complementarity, which we intend to address in future work. This information will grow in importance when higher-energy LHC data are analyzed, since the increased phase space will further improve the sensitivity to dimension-6 operators.

Note added. We thank A. Knochel and the authors of ref. [137] for pointing out to us that the previous version of this paper underestimated the ATLAS p_V^T constraints due to a misinterpretation of the expected number of SM events in table 5 of ref. [110], which actually corresponds to a best fit signal strength of 0.2. Normalising instead to a signal

strength of 1.0 yields improved constraints competitive with those of LEP, in agreement with comparable results in [137].

Acknowledgments

A   D0 $H + V$ analysis

A.1 $p\bar{p} \rightarrow Zh \rightarrow l\bar{l}b\bar{b}$

The event selection for the 2-lepton channel is taken from [133]. The basic cuts for di-electrons are $p_T > 15$, $|\eta| < 15$ and at least one electron with $|\eta| < 1.1$, and for di-muons are $p_T > 10\,\text{GeV}$, $|\eta| < 2$ and at least one muon with $p_T > 15\,\text{GeV}, |\eta| < 1.5$. The muons have an isolation cut that requires them to be separated from all jets by $\Delta R = \sqrt{\Delta\eta^2 + \Delta\phi^2} > 0.5$.

The "pretag" cuts are then applied to keep only events with $70 < M_{ll} < 110\,\text{GeV}$ and at least two jets having $p_T > 20\,\text{GeV}$ and $|\eta| < 2.5$. The final selection step is b-tagging the jets according to "loose" and "tight" categories, with at least one tight and one loose b-tagged jet. We simulate this double-tagged (DT) requirement by using the efficiencies reported as a function of p_T in [134]. Fitting to figure 6a and 6b in that reference yields the following formula for the loose and tight efficiencies ϵ:

$$\epsilon_{\text{loose}} = a_{\text{loose}} e^{-\frac{p_T}{600}} \tanh(0.020 p_T + 0.77) \,,$$

$$\epsilon_{\text{tight}} = a_{\text{tight}} e^{-\frac{p_T}{360}} \tanh(0.029 p_T + 0.34) \,,$$

where the coefficients $a_{\text{loose}} = 0.79, a_{\text{tight}} = 0.70$ in the region $|\eta| < 1.5$ and $a_{\text{loose}} = 0.67, a_{\text{tight}} = 0.58$ for $|\eta| > 1.5$, the efficiency being fairly flat as a function of η in these regions.

Finally we set the `Delphes` ECAL and HCAL resolutions as functions of energy E to $0.01E + 0.2\sqrt{E} + 0.25$ and $0.050E + 0.8\sqrt{E}$ respectively. The same expression is used for the ECAL electron energy resolution.

After running our simulation we obtain the number of signal events by multiplying the cross-section given by `MadGraph` with the efficiency after cuts and reweighting by a k-factor of 1.5 as an overall normalization. We find the resulting number of pretag and DT signal events for a SM Higgs to be 8.6 and 3.1 respectively, in agreement with the numbers listed in table 3 of [133]. We have also verified that we reproduce well the distribution of $H + V$ invariant masses for the SM Higgs signal given by D0 in figure 2c of [73].

A.2 $p\bar{p} \to Wh \to l\nu b\bar{b}$

We implement the cuts listed in [135] by requiring one electron (muon) with $p_T > 15$ and $|\eta| < 2.5\,(2.0)$, and by requiring two jets with $p_T > 20\,\mathrm{GeV}$ and $|\eta| < 2.5$. The muon is required to be isolated from all jets by $\Delta R > 0.5$. Finally, the transverse mass M_T^W, defined as $2p_T^l \not{E}_T(1 - \cos\Delta\phi(l, \not{E}_T))$, must satisfy $M_T^W > 40\mathrm{GeV} - 0.5\not{E}_T$. This defines the pretag events with the b-tag cut then applied as described previously. Running the simulation with the cross-section times efficiency reweighted by a k-factor of 1.7 gives good agreement with the expected numbers of pretag and final events given in table 1 of [135].

A.3 $p\bar{p} \to Zh \to \nu\bar{\nu} b\bar{b}$

Following [136], we select events containing two jets with $p_T > 20\,\mathrm{GeV}$ and $|\eta| < 2.5$, whose opening angle is $\Delta\phi < 165°$, and apply a missing transverse energy cut $\not{E}_T > 40\,\mathrm{GeV}$. The jets are furthermore required to have the scalar sum of the their transverse momenta larger than $80\,\mathrm{GeV}$. We also reject events with an isolated muon or electron having $p_T > 15\,\mathrm{GeV}$. We verified that the resulting numbers of events both before and after b-tag cuts agree within errors with the numbers given in table 1 of [136] without any reweighting.

B   ATLAS $H + V$ analysis

The implementation of this analysis follows the cuts given in [110].

B.1 $p\bar{p} \to Zh \to l\bar{l}b\bar{b}$

We select events with exactly 2 muons (electrons) satisfying $|\eta| < 2.5\,(2.47)$ and $83 < M_{ll} < 99\,\mathrm{GeV}$. A missing transverse energy cut of E_T^{miss} is applied. There must be only 2 b-tagged jets with the higher-p_T jet $> 45\,\mathrm{GeV}$ and $p_T > 20\,\mathrm{GeV}$ for the other jet, and both with $|\eta| < 2.5$. Finally we place a ΔR cut on the angle between the two jets which varies depending on the p_T^V bin (see table 2 in [110]). The transverse momentum p_T^V of the vector boson is reconstructed using the vector sum of the transverse components of the two leptons.

We simulate events at the $8\,\mathrm{TeV}$ LHC with the resulting distribution in the p_T^V bins used by ATLAS. We reweight the cross-section so as to normalise the number of signal events in each bin to the expected SM count from table 5 of [110].

B.2 $p\bar{p} \to Wh \to l\nu b\bar{b}$

In this sub-channel we select exactly one muon (electron) with $|\eta| < 2.5\,(2.47)$ and $E_T > 25\,\mathrm{GeV}$. The missing transverse energy requirement is $E_T^{\mathrm{miss}} > 25\,(50)$ for p_T^V less (greater) than $200\,\mathrm{GeV}$. The invariant transverse mass m_T^W is required to be less than $120\,\mathrm{GeV}$, and for $p_T^V < 160\,\mathrm{GeV}$ it must also be greater than $40\,\mathrm{GeV}$. The p_T^V transverse momentum is in this case the vector sum of the transverse components of the lepton and missing E_T. The jet requirements are the same as for the 2-lepton case, and we have normalised our number of events after simulation in the same way as above.

B.3 $p\bar{p} \to Zh \to \nu\bar{\nu}b\bar{b}$

Here we require no leptons that pass the other criterias and a large missing transverse energy of $E_T^{\text{miss}} > 120\,\text{GeV}$ with $p_T^{\text{miss}} > 30\,\text{GeV}$ and an angle between the two of $\Delta\phi < \pi/2$. The azimuthal angle between the E_T^{miss} and the vector sum of the jets must be $\Delta\phi > 4.8$, as well as $\Delta\phi > 1.5$ with the nearest jet. The other jet cuts and ΔR requirements as a function of p_T^V are also the same here, with the p_T^V identified as the E_{miss}^T. We again normalize the number of signal events to the SM expectation from table 5 of [110].

Open Access. This article is distributed under the terms of the Creative Commons Attribution License (CC-BY 4.0), which permits any use, distribution and reproduction in any medium, provided the original author(s) and source are credited.

References

[1] ATLAS collaboration, *Observation of a new particle in the search for the Standard Model Higgs boson with the ATLAS detector at the LHC*, *Phys. Lett.* **B 716** (2012) 1 [arXiv:1207.7214] [INSPIRE].

[2] CMS collaboration, *Observation of a new boson at a mass of 125 GeV with the CMS experiment at the LHC*, *Phys. Lett.* **B 716** (2012) 30 [arXiv:1207.7235] [INSPIRE].

[3] CMS collaboration, *Observation of a new boson with mass near 125 GeV in pp collisions at $\sqrt{s} = 7$ and 8 TeV*, *JHEP* **06** (2013) 081 [arXiv:1303.4571] [INSPIRE].

[4] ATLAS collaboration, *Constraints on New Phenomena via Higgs Coupling Measurements with the ATLAS Detector*, ATLAS-CONF-2014-010.

[5] M. Baak, M. Goebel, J. Haller, A. Hoecker, D. Ludwig et al., *Updated Status of the Global Electroweak Fit and Constraints on New Physics*, *Eur. Phys. J.* **C 72** (2012) 2003 [arXiv:1107.0975] [INSPIRE].

[6] D. Carmi, A. Falkowski, E. Kuflik and T. Volansky, *Interpreting LHC Higgs Results from Natural New Physics Perspective*, *JHEP* **07** (2012) 136 [arXiv:1202.3144] [INSPIRE].

[7] A. Azatov, R. Contino and J. Galloway, *Model-Independent Bounds on a Light Higgs*, *JHEP* **04** (2012) 127 [*Erratum ibid.* **1304** (2013) 140] [arXiv:1202.3415] [INSPIRE].

[8] J.R. Espinosa, C. Grojean, M. Muhlleitner and M. Trott, *Fingerprinting Higgs Suspects at the LHC*, *JHEP* **05** (2012) 097 [arXiv:1202.3697] [INSPIRE].

[9] P.P. Giardino, K. Kannike, M. Raidal and A. Strumia, *Reconstructing Higgs boson properties from the LHC and Tevatron data*, *JHEP* **06** (2012) 117 [arXiv:1203.4254] [INSPIRE].

[10] T. Li, X. Wan, Y.-k. Wang and S.-h. Zhu, *Constraints on the Universal Varying Yukawa Couplings: from SM-like to Fermiophobic*, *JHEP* **09** (2012) 086 [arXiv:1203.5083] [INSPIRE].

[11] M. Rauch, *Determination of Higgs-boson couplings (SFitter)*, arXiv:1203.6826 [INSPIRE].

[12] J. Ellis and T. You, *Global Analysis of Experimental Constraints on a Possible Higgs-Like Particle with Mass 125 GeV*, *JHEP* **06** (2012) 140 [arXiv:1204.0464] [INSPIRE].

[13] A. Azatov, R. Contino, D. Del Re, J. Galloway, M. Grassi et al., *Determining Higgs couplings with a model-independent analysis of h → γγ*, *JHEP* **06** (2012) 134 [arXiv:1204.4817] [INSPIRE].

[14] M. Klute, R. Lafaye, T. Plehn, M. Rauch and D. Zerwas, *Measuring Higgs Couplings from LHC Data*, *Phys. Rev. Lett.* **109** (2012) 101801 [arXiv:1205.2699] [INSPIRE].

[15] L. Wang and X.-F. Han, *The recent Higgs boson data and Higgs triplet model with vector-like quark*, *Phys. Rev.* **D 86** (2012) 095007 [arXiv:1206.1673] [INSPIRE].

[16] D. Carmi, A. Falkowski, E. Kuflik and T. Volansky, *Interpreting the 125 GeV Higgs*, *Nuovo Cim.* **C 035** (2012) 315 [arXiv:1206.4201] [INSPIRE].

[17] M.J. Dolan, C. Englert and M. Spannowsky, *Higgs self-coupling measurements at the LHC*, *JHEP* **10** (2012) 112 [arXiv:1206.5001] [INSPIRE].

[18] J. Chang, K. Cheung, P.-Y. Tseng and T.-C. Yuan, *Distinguishing Various Models of the 125 GeV Boson in Vector Boson Fusion*, *JHEP* **12** (2012) 058 [arXiv:1206.5853] [INSPIRE].

[19] S. Chang, C.A. Newby, N. Raj and C. Wanotayaroj, *Revisiting Theories with Enhanced Higgs Couplings to Weak Gauge Bosons*, *Phys. Rev.* **D 86** (2012) 095015 [arXiv:1207.0493] [INSPIRE].

[20] I. Low, J. Lykken and G. Shaughnessy, *Have We Observed the Higgs (Imposter)?*, *Phys. Rev.* **D 86** (2012) 093012 [arXiv:1207.1093] [INSPIRE].

[21] J. Ellis and T. You, *Global Analysis of the Higgs Candidate with Mass 125 GeV*, *JHEP* **09** (2012) 123 [arXiv:1207.1693] [INSPIRE].

[22] P.P. Giardino, K. Kannike, M. Raidal and A. Strumia, *Is the resonance at 125 GeV the Higgs boson?*, *Phys. Lett.* **B 718** (2012) 469 [arXiv:1207.1347] [INSPIRE].

[23] M. Montull and F. Riva, *Higgs discovery: the beginning or the end of natural EWSB?*, *JHEP* **11** (2012) 018 [arXiv:1207.1716] [INSPIRE].

[24] J.R. Espinosa, C. Grojean, M. Muhlleitner and M. Trott, *First Glimpses at Higgs' face*, *JHEP* **12** (2012) 045 [arXiv:1207.1717] [INSPIRE].

[25] D. Carmi, A. Falkowski, E. Kuflik, T. Volansky and J. Zupan, *Higgs After the Discovery: A Status Report*, *JHEP* **10** (2012) 196 [arXiv:1207.1718] [INSPIRE].

[26] S. Banerjee, S. Mukhopadhyay and B. Mukhopadhyaya, *New Higgs interactions and recent data from the LHC and the Tevatron*, *JHEP* **10** (2012) 062 [arXiv:1207.3588] [INSPIRE].

[27] F. Bonnet, T. Ota, M. Rauch and W. Winter, *Interpretation of precision tests in the Higgs sector in terms of physics beyond the Standard Model*, *Phys. Rev.* **D 86** (2012) 093014 [arXiv:1207.4599] [INSPIRE].

[28] T. Plehn and M. Rauch, *Higgs Couplings after the Discovery*, *Europhys. Lett.* **100** (2012) 11002 [arXiv:1207.6108] [INSPIRE].

[29] A. Djouadi, *Precision Higgs coupling measurements at the LHC through ratios of production cross sections*, *Eur. Phys. J.* **C 73** (2013) 2498 [arXiv:1208.3436] [INSPIRE].

[30] B. Batell, S. Gori and L.-T. Wang, *Higgs Couplings and Precision Electroweak Data*, *JHEP* **01** (2013) 139 [arXiv:1209.6382] [INSPIRE].

[31] G. Moreau, *Constraining extra-fermion(s) from the Higgs boson data*, *Phys. Rev.* **D 87** (2013) 015027 [arXiv:1210.3977] [INSPIRE].

[32] G. Cacciapaglia, A. Deandrea, G.D. La Rochelle and J.-B. Flament, *Higgs couplings beyond the Standard Model*, *JHEP* **03** (2013) 029 [`arXiv:1210.8120`] [inSPIRE].

[33] E. Masso and V. Sanz, *Limits on Anomalous Couplings of the Higgs to Electroweak Gauge Bosons from LEP and LHC*, *Phys. Rev.* **D 87** (2013) 033001 [`arXiv:1211.1320`] [inSPIRE].

[34] R.T. D'Agnolo, E. Kuflik and M. Zanetti, *Fitting the Higgs to Natural SUSY*, *JHEP* **03** (2013) 043 [`arXiv:1212.1165`] [inSPIRE].

[35] A. Azatov and J. Galloway, *Electroweak Symmetry Breaking and the Higgs Boson: Confronting Theories at Colliders*, *Int. J. Mod. Phys.* **A 28** (2013) 1330004 [`arXiv:1212.1380`] [inSPIRE].

[36] G. Bhattacharyya, D. Das and P.B. Pal, *Modified Higgs couplings and unitarity violation*, *Phys. Rev.* **D 87** (2013) 011702 [`arXiv:1212.4651`] [inSPIRE].

[37] D. Choudhury, R. Islam and A. Kundu, *Anomalous Higgs Couplings as a Window to New Physics*, *Phys. Rev.* **D 88** (2013) 013014 [`arXiv:1212.4652`] [inSPIRE].

[38] R.S. Gupta, M. Montull and F. Riva, *SUSY Faces its Higgs Couplings*, *JHEP* **04** (2013) 132 [`arXiv:1212.5240`] [inSPIRE].

[39] G. Bélanger, B. Dumont, U. Ellwanger, J.F. Gunion and S. Kraml, *Higgs Couplings at the End of 2012*, *JHEP* **02** (2013) 053 [`arXiv:1212.5244`] [inSPIRE].

[40] K. Cheung, J.S. Lee and P.-Y. Tseng, *Higgs Precision (Higgcision) Era begins*, *JHEP* **05** (2013) 134 [`arXiv:1302.3794`] [inSPIRE].

[41] A. Falkowski, F. Riva and A. Urbano, *Higgs at last*, *JHEP* **11** (2013) 111 [`arXiv:1303.1812`] [inSPIRE].

[42] P.P. Giardino, K. Kannike, I. Masina, M. Raidal and A. Strumia, *The universal Higgs fit*, *JHEP* **05** (2014) 046 [`arXiv:1303.3570`] [inSPIRE].

[43] J. Ellis and T. You, *Updated Global Analysis of Higgs Couplings*, *JHEP* **06** (2013) 103 [`arXiv:1303.3879`] [inSPIRE].

[44] S. Banerjee, S. Mukhopadhyay and B. Mukhopadhyaya, *Higher dimensional operators and LHC Higgs data : the role of modified kinematics*, *Phys. Rev.* **D 89** (2014) 053010 [`arXiv:1308.4860`] [inSPIRE].

[45] J. Ellis, V. Sanz and T. You, *Prima Facie Evidence against Spin-Two Higgs Impostors*, *Phys. Lett.* **B 726** (2013) 244 [`arXiv:1211.3068`] [inSPIRE].

[46] J. Ellis and D.S. Hwang, *Does the 'Higgs' have Spin Zero?*, *JHEP* **09** (2012) 071 [`arXiv:1202.6660`] [inSPIRE].

[47] A. Alves, *Is the New Resonance Spin 0 or 2? Taking a Step Forward in the Higgs Boson Discovery*, *Phys. Rev.* **D 86** (2012) 113010 [`arXiv:1209.1037`] [inSPIRE].

[48] J. Ellis, R. Fok, D.S. Hwang, V. Sanz and T. You, *Distinguishing 'Higgs' spin hypotheses using $\gamma\gamma$ and WW^* decays*, *Eur. Phys. J.* **C 73** (2013) 2488 [`arXiv:1210.5229`] [inSPIRE].

[49] Y. Gao, A.V. Gritsan, Z. Guo, K. Melnikov, M. Schulze et al., *Spin determination of single-produced resonances at hadron colliders*, *Phys. Rev.* **D 81** (2010) 075022 [`arXiv:1001.3396`] [inSPIRE].

[50] M.C. Kumar, P. Mathews, A.A. Pankov, N. Paver, V. Ravindran et al., *Spin-analysis of s-channel diphoton resonances at the LHC*, *Phys. Rev.* **D 84** (2011) 115008 [`arXiv:1108.3764`] [inSPIRE].

[51] S.Y. Choi, D.J. Miller, M.M. Muhlleitner and P.M. Zerwas, *Identifying the Higgs spin and parity in decays to Z pairs*, *Phys. Lett.* **B 553** (2003) 61 [hep-ph/0210077] [INSPIRE].

[52] K. Odagiri, *On azimuthal spin correlations in Higgs plus jet events at LHC*, *JHEP* **03** (2003) 009 [hep-ph/0212215] [INSPIRE].

[53] C.P. Buszello, I. Fleck, P. Marquard and J.J. van der Bij, *Prospective analysis of spin- and CP-sensitive variables in H → Z Z → l(1)+ l(1)- l(2)+ l(2)- at the LHC*, *Eur. Phys. J.* **C 32** (2004) 209 [hep-ph/0212396] [INSPIRE].

[54] A. Djouadi, *The Anatomy of electro-weak symmetry breaking. I: The Higgs boson in the standard model*, *Phys. Rept.* **457** (2008) 1 [hep-ph/0503172] [INSPIRE].

[55] C.P. Buszello and P. Marquard, *Determination of spin and CP of the Higgs boson from WBF*, hep-ph/0603209 [INSPIRE].

[56] A. Bredenstein, A. Denner, S. Dittmaier and M.M. Weber, *Precise predictions for the Higgs-boson decay H → WW/ZZ → 4 leptons*, *Phys. Rev.* **D 74** (2006) 013004 [hep-ph/0604011] [INSPIRE].

[57] P.S. Bhupal Dev, A. Djouadi, R.M. Godbole, M.M. Muhlleitner and S.D. Rindani, *Determining the CP properties of the Higgs boson*, *Phys. Rev. Lett.* **100** (2008) 051801 [arXiv:0707.2878] [INSPIRE].

[58] R.M. Godbole, D.J. Miller and M.M. Muhlleitner, *Aspects of CP-violation in the H ZZ coupling at the LHC*, *JHEP* **12** (2007) 031 [arXiv:0708.0458] [INSPIRE].

[59] K. Hagiwara, Q. Li and K. Mawatari, *Jet angular correlation in vector-boson fusion processes at hadron colliders*, *JHEP* **07** (2009) 101 [arXiv:0905.4314] [INSPIRE].

[60] A. De Rujula, J. Lykken, M. Pierini, C. Rogan and M. Spiropulu, *Higgs look-alikes at the LHC*, *Phys. Rev.* **D 82** (2010) 013003 [arXiv:1001.5300] [INSPIRE].

[61] C. Englert, C. Hackstein and M. Spannowsky, *Measuring spin and CP from semi-hadronic ZZ decays using jet substructure*, *Phys. Rev.* **D 82** (2010) 114024 [arXiv:1010.0676] [INSPIRE].

[62] U. De Sanctis, M. Fabbrichesi and A. Tonero, *Telling the spin of the 'Higgs boson' at the LHC*, *Phys. Rev.* **D 84** (2011) 015013 [arXiv:1103.1973] [INSPIRE].

[63] V. Barger and P. Huang, *Higgs boson finder and mass estimator: The Higgs boson to WW to leptons decay channel at the LHC*, *Phys. Rev.* **D 84** (2011) 093001 [arXiv:1107.4131] [INSPIRE].

[64] S. Bolognesi, Y. Gao, A.V. Gritsan, K. Melnikov, M. Schulze et al., *On the spin and parity of a single-produced resonance at the LHC*, *Phys. Rev.* **D 86** (2012) 095031 [arXiv:1208.4018] [INSPIRE].

[65] R. Boughezal, T.J. LeCompte and F. Petriello, *Single-variable asymmetries for measuring the 'Higgs' boson spin and CP properties*, arXiv:1208.4311 [INSPIRE].

[66] D. Stolarski and R. Vega-Morales, *Directly Measuring the Tensor Structure of the Scalar Coupling to Gauge Bosons*, *Phys. Rev.* **D 86** (2012) 117504 [arXiv:1208.4840] [INSPIRE].

[67] S.Y. Choi, M.M. Muhlleitner and P.M. Zerwas, *Theoretical Basis of Higgs-Spin Analysis in H → γγ and Zγ Decays*, *Phys. Lett.* **B 718** (2013) 1031 [arXiv:1209.5268] [INSPIRE].

[68] P. Avery, D. Bourilkov, M. Chen, T. Cheng, A. Drozdetskiy et al., *Precision studies of the Higgs boson decay channel H → ZZ → 4l with MEKD*, *Phys. Rev.* **D 87** (2013) 055006 [arXiv:1210.0896] [INSPIRE].

[69] C.-Q. Geng, D. Huang, Y. Tang and Y.-L. Wu, *Note on 125 GeV Spin-2 particle*, *Phys. Lett.* **B 719** (2013) 164 [arXiv:1210.5103] [inSPIRE].

[70] A. Menon, T. Modak, D. Sahoo, R. Sinha and H.-Y. Cheng, *Inferring the nature of the boson at 125-126 GeV*, *Phys. Rev.* **D 89** (2014) 095021 [arXiv:1301.5404] [inSPIRE].

[71] CMS collaboration, *Study of the Mass and Spin-Parity of the Higgs Boson Candidate Via Its Decays to Z Boson Pairs*, *Phys. Rev. Lett.* **110** (2013) 081803 [arXiv:1212.6639] [inSPIRE].

[72] ATLAS collaboration, *Evidence for the spin-0 nature of the Higgs boson using ATLAS data*, *Phys. Lett.* **B 726** (2013) 120 [arXiv:1307.1432] [inSPIRE].

[73] D0 collaboration, *Constraints on the $J^P = 2^+$ hypothesis for the 125 GeV boson in $W/Z + b\bar{b}$ final states at the D0 Experiment*, D0 Note 6387-CONF.

[74] W. Buchmüller and D. Wyler, *Effective Lagrangian Analysis of New Interactions and Flavor Conservation*, *Nucl. Phys.* **B 268** (1986) 621 [inSPIRE].

[75] K. Hagiwara, S. Ishihara, R. Szalapski and D. Zeppenfeld, *Low-energy effects of new interactions in the electroweak boson sector*, *Phys. Rev.* **D 48** (1993) 2182 [inSPIRE].

[76] K. Hagiwara, R. Szalapski and D. Zeppenfeld, *Anomalous Higgs boson production and decay*, *Phys. Lett.* **B 318** (1993) 155 [hep-ph/9308347] [inSPIRE].

[77] B. Grzadkowski, M. Iskrzynski, M. Misiak and J. Rosiek, *Dimension-Six Terms in the Standard Model Lagrangian*, *JHEP* **10** (2010) 085 [arXiv:1008.4884] [inSPIRE].

[78] M.B. Einhorn and J. Wudka, *The Bases of Effective Field Theories*, *Nucl. Phys.* **B 876** (2013) 556 [arXiv:1307.0478] [inSPIRE].

[79] S. Willenbrock and C. Zhang, *Effective Field Theory Beyond the Standard Model*, arXiv:1401.0470 [inSPIRE].

[80] F. Bonnet, M.B. Gavela, T. Ota and W. Winter, *Anomalous Higgs couplings at the LHC and their theoretical interpretation*, *Phys. Rev.* **D 85** (2012) 035016 [arXiv:1105.5140] [inSPIRE].

[81] T. Corbett, O.J.P. Eboli, J. Gonzalez-Fraile and M.C. Gonzalez-Garcia, *Constraining anomalous Higgs interactions*, *Phys. Rev.* **D 86** (2012) 075013 [arXiv:1207.1344] [inSPIRE].

[82] W.-F. Chang, W.-P. Pan and F. Xu, *Effective gauge-Higgs operators analysis of new physics associated with the Higgs boson*, *Phys. Rev.* **D 88** (2013) 033004 [arXiv:1303.7035] [inSPIRE].

[83] A. Hayreter and G. Valencia, *Constraints on anomalous color dipole operators from Higgs boson production at the LHC*, *Phys. Rev.* **D 88** (2013) 034033 [arXiv:1304.6976] [inSPIRE].

[84] J. Elias-Miro, J.R. Espinosa, E. Masso and A. Pomarol, *Higgs windows to new physics through $D = 6$ operators: constraints and one-loop anomalous dimensions*, *JHEP* **11** (2013) 066 [arXiv:1308.1879] [inSPIRE].

[85] S. Banerjee, S. Mukhopadhyay and B. Mukhopadhyaya, *Higher dimensional operators and LHC Higgs data: the role of modified kinematics*, *Phys. Rev.* **D 89** (2014) 053010 [arXiv:1308.4860] [inSPIRE].

[86] E. Boos, V. Bunichev, M. Dubinin and Y. Kurihara, *Higgs boson signal at complete tree level in the SM extension by dimension-six operators*, *Phys. Rev.* **D 89** (2014) 035001 [arXiv:1309.5410] [inSPIRE].

[87] M. Dahiya, S. Dutta and R. Islam, *Unitarizing VV Scattering in Light Higgs Scenarios*, arXiv:1311.4523 [InSPIRE].

[88] J.S. Gainer, J. Lykken, K.T. Matchev, S. Mrenna and M. Park, *Beyond Geolocating: Constraining Higher Dimensional Operators in $H \to 4\ell$ with Off-Shell Production and More*, arXiv:1403.4951 [InSPIRE].

[89] E. Masso and V. Sanz, *Limits on Anomalous Couplings of the Higgs to Electroweak Gauge Bosons from LEP and LHC*, *Phys. Rev.* **D 87** (2013) 033001 [arXiv:1211.1320] [InSPIRE].

[90] Z. Han and W. Skiba, *Effective theory analysis of precision electroweak data*, *Phys. Rev.* **D 71** (2005) 075009 [hep-ph/0412166] [InSPIRE].

[91] T. Corbett, O.J.P. Eboli, J. Gonzalez-Fraile and M.C. Gonzalez-Garcia, *Robust Determination of the Higgs Couplings: Power to the Data*, *Phys. Rev.* **D 87** (2013) 015022 [arXiv:1211.4580] [InSPIRE].

[92] B. Dumont, S. Fichet and G. von Gersdorff, *A Bayesian view of the Higgs sector with higher dimensional operators*, *JHEP* **07** (2013) 065 [arXiv:1304.3369] [InSPIRE].

[93] A. Pomarol and F. Riva, *Towards the Ultimate SM Fit to Close in on Higgs Physics*, *JHEP* **01** (2014) 151 [arXiv:1308.2803] [InSPIRE].

[94] S. Alam, S. Dawson and R. Szalapski, *Low-energy constraints on new physics revisited*, *Phys. Rev.* **D 57** (1998) 1577 [hep-ph/9706542] [InSPIRE].

[95] A. De Rujula, M.B. Gavela, P. Hernández and E. Masso, *The Selfcouplings of vector bosons: Does LEP-1 obviate LEP-2?*, *Nucl. Phys.* **B 384** (1992) 3 [InSPIRE].

[96] H. Mebane, N. Greiner, C. Zhang and S. Willenbrock, *Constraints on Electroweak Effective Operators at One Loop*, *Phys. Rev.* **D 88** (2013) 015028 [arXiv:1306.3380] [InSPIRE].

[97] T. Corbett, O.J.P. Éboli, J. Gonzalez-Fraile and M.C. Gonzalez-Garcia, *Determining Triple Gauge Boson Couplings from Higgs Data*, *Phys. Rev. Lett.* **111** (2013) 011801 [arXiv:1304.1151] [InSPIRE].

[98] A. Falkowski, S. Fichet, K. Mohan, F. Riva and V. Sanz, *Triple gauge couplings revisited*, contribution to the Les Houches 2013 proceedings, to appear.

[99] C. Grojean, E.E. Jenkins, A.V. Manohar and M. Trott, *Renormalization Group Scaling of Higgs Operators and $\Gamma(h \to \gamma\gamma)$*, *JHEP* **04** (2013) 016 [arXiv:1301.2588] [InSPIRE].

[100] J. Elias-Miró, J.R. Espinosa, E. Masso and A. Pomarol, *Renormalization of dimension-six operators relevant for the Higgs decays $h \to \gamma\gamma, \gamma Z$*, *JHEP* **08** (2013) 033 [arXiv:1302.5661] [InSPIRE].

[101] J. Elias-Miro, J.R. Espinosa, E. Masso and A. Pomarol, *Higgs windows to new physics through $D = 6$ operators: constraints and one-loop anomalous dimensions*, *JHEP* **11** (2013) 066 [arXiv:1308.1879] [InSPIRE].

[102] E.E. Jenkins, A.V. Manohar and M. Trott, *Renormalization Group Evolution of the Standard Model Dimension Six Operators I: Formalism and lambda Dependence*, *JHEP* **10** (2013) 087 [arXiv:1308.2627] [InSPIRE].

[103] E.E. Jenkins, A.V. Manohar and M. Trott, *Renormalization Group Evolution of the Standard Model Dimension Six Operators II: Yukawa Dependence*, *JHEP* **01** (2014) 035 [arXiv:1310.4838] [InSPIRE].

[104] R. Alonso, E.E. Jenkins, A.V. Manohar and M. Trott, *Renormalization Group Evolution of the Standard Model Dimension Six Operators III: Gauge Coupling Dependence and Phenomenology*, *JHEP* **04** (2014) 159 [arXiv:1312.2014] [INSPIRE].

[105] J. Elias-Miró, C. Grojean, R.S. Gupta and D. Marzocca, *Scaling and tuning of EW and Higgs observables*, *JHEP* **05** (2014) 019 [arXiv:1312.2928] [INSPIRE].

[106] C.-Y. Chen, S. Dawson and C. Zhang, *Electroweak Effective Operators and Higgs Physics*, *Phys. Rev.* **D 89** (2014) 015016 [arXiv:1311.3107] [INSPIRE].

[107] H. Mebane, N. Greiner, C. Zhang and S. Willenbrock, *Constraints on Electroweak Effective Operators at One Loop*, *Phys. Rev.* **D 88** (2013) 015028 [arXiv:1306.3380] [INSPIRE].

[108] B. Henning, X. Lu and H. Murayama, *What do precision Higgs measurements buy us?*, arXiv:1404.1058 [INSPIRE].

[109] D0 collaboration, V.M. Abazov et al., *Combined search for the standard model Higgs boson decaying to $b\bar{b}$ using the D0 Run II data set*, *Phys. Rev. Lett.* **109** (2012) 121802 [arXiv:1207.6631] [INSPIRE].

[110] ATLAS collaboration, *Search for the bb decay of the Standard Model Higgs boson in associated W/ZH production with the ATLAS detector*, ATLAS-CONF-2013-079.

[111] J. Ellis, V. Sanz and T. You, *Associated Production Evidence against Higgs Impostors and Anomalous Couplings*, *Eur. Phys. J.* **C 73** (2013) 2507 [arXiv:1303.0208] [INSPIRE].

[112] G. Isidori and M. Trott, *Higgs form factors in Associated Production*, *JHEP* **02** (2014) 082 [arXiv:1307.4051] [INSPIRE].

[113] G.F. Giudice, C. Grojean, A. Pomarol and R. Rattazzi, *The Strongly-Interacting Light Higgs*, *JHEP* **06** (2007) 045 [hep-ph/0703164] [INSPIRE].

[114] R. Contino, C. Grojean, M. Moretti, F. Piccinini and R. Rattazzi, *Strong Double Higgs Production at the LHC*, *JHEP* **05** (2010) 089 [arXiv:1002.1011] [INSPIRE].

[115] R. Contino, *The Higgs as a Composite Nambu-Goldstone Boson*, arXiv:1005.4269 [INSPIRE].

[116] R. Grober and M. Muhlleitner, *Composite Higgs Boson Pair Production at the LHC*, *JHEP* **06** (2011) 020 [arXiv:1012.1562] [INSPIRE].

[117] A. Alloul, B. Fuks and V. Sanz, *Phenomenology of the Higgs Effective Lagrangian via FeynRules*, *JHEP* **04** (2014) 110 [arXiv:1310.5150] [INSPIRE].

[118] J. Alwall, M. Herquet, F. Maltoni, O. Mattelaer and T. Stelzer, *MadGraph 5 : Going Beyond*, *JHEP* **06** (2011) 128 [arXiv:1106.0522] [INSPIRE].

[119] T. Sjöstrand, S. Mrenna and P.Z. Skands, *PYTHIA 6.4 Physics and Manual*, *JHEP* **05** (2006) 026 [hep-ph/0603175] [INSPIRE].

[120] DELPHES 3 collaboration, J. de Favereau et al., *DELPHES 3, A modular framework for fast simulation of a generic collider experiment*, *JHEP* **02** (2014) 057 [arXiv:1307.6346] [INSPIRE].

[121] J. Ellis, D.S. Hwang, V. Sanz and T. You, *A Fast Track towards the 'Higgs' Spin and Parity*, *JHEP* **11** (2012) 134 [arXiv:1208.6002] [INSPIRE].

[122] V. Sanz and C. Williams, in preparation.

[123] J.M. Campbell and R.K. Ellis, *MCFM for the Tevatron and the LHC*, *Nucl. Phys. Proc. Suppl.* **205** (2010) 10 [arXiv:1007.3492] [INSPIRE].

[124] J.M. Campbell, *W/Z + B, $\bar{B}$/ jets at NLO using the Monte Carlo MCFM*, hep-ph/0105226 [INSPIRE].

[125] J.M. Campbell, R.K. Ellis and C. Williams, *Vector boson pair production at the LHC*, *JHEP* **07** (2011) 018 [arXiv:1105.0020] [INSPIRE].

[126] R. Contino, M. Ghezzi, C. Grojean, M. Muhlleitner and M. Spira, *Effective Lagrangian for a light Higgs-like scalar*, *JHEP* **07** (2013) 035 [arXiv:1303.3876] [INSPIRE].

[127] R. Contino, M. Ghezzi, C. Grojean, M. Muhlleitner and M. Spira, *eHDECAY: an Implementation of the Higgs Effective Lagrangian into HDECAY*, arXiv:1403.3381 [INSPIRE].

[128] F. Boudjema, G. Cacciapaglia, K. Cranmer, G. Dissertori, A. Deandrea et al., *On the presentation of the LHC Higgs Results*, arXiv:1307.5865 [INSPIRE].

[129] ATLAS collaboration, *Measurements of Higgs boson production and couplings in diboson final states with the ATLAS detector at the LHC*, *Phys. Lett.* **B 726** (2013) 88 [arXiv:1307.1427] [INSPIRE].

[130] ATLAS collaboration, *Combined coupling measurements of the Higgs-like boson with the ATLAS detector using up to 25 fb^{-1} of proton-proton collision data*, ATLAS-CONF-2013-034.

[131] CMS collaboration, *Combination of standard model Higgs boson searches and measurements of the properties of the new boson with a mass near 125 GeV*, CMS-PAS-HIG-13-005.

[132] A. Azatov, R. Contino and J. Galloway, *Model-Independent Bounds on a Light Higgs*, *JHEP* **04** (2012) 127 [*Erratum ibid.* **1304** (2013) 140] [arXiv:1202.3415] [INSPIRE].

[133] D0 collaboration, V.M. Abazov et al., *Search for $ZH \to \ell^+\ell^- b\bar{b}$ production in 9.7 fb^{-1} of $p\bar{p}$ collisions with the D0 detector*, *Phys. Rev.* **D 88** (2013) 052010 [arXiv:1303.3276] [INSPIRE].

[134] D0 collaboration, V.M. Abazov et al., *Improved b quark jet identification at the D0 experiment*, arXiv:1312.7623 [INSPIRE].

[135] D0 collaboration, V.M. Abazov et al., *Search for the standard model Higgs boson in $\ell\nu$ + jets final states in 9.7 fb^{-1} of $p\bar{p}$ collisions with the D0 detector*, *Phys. Rev.* **D 88** (2013) 052008 [arXiv:1301.6122] [INSPIRE].

[136] D0 collaboration, V.M. Abazov et al., *Search for the standard model Higgs boson in the $ZH \to \nu\bar{\nu}b\bar{b}$ channel in 9.5 fb^{-1} of $p\bar{p}$ collisions at $\sqrt{s} = 1.96$ TeV*, *Phys. Lett.* **B 716** (2012) 285 [arXiv:1207.5689] [INSPIRE].

[137] A. Biekoetter, A. Knochel, M. Kraemer, D. Liu and F. Riva, *Vices and Virtues of Higgs EFTs at Large Energy*, arXiv:1406.7320 [INSPIRE].